

Direct Measurement of Superluminal Group Velocity and Signal Velocity in an Optical Fiber

Nicolas Brunner, Valerio Scarani, Mark Wegmüller, Matthieu Legré, and Nicolas Gisin

Group of Applied Physics, University of Geneva, 20 rue de l'École-de-Médecine, CH-1211 Geneva 4, Switzerland

(Received 21 July 2004; published 11 November 2004)

We present an easy way of observing superluminal group velocities using a birefringent optical fiber and other standard devices. In the theoretical analysis, we show that the optical properties of the setup can be described using the notion of “weak value.” The experiment shows that the group velocity can indeed exceed c in the fiber; and we report the first direct observation of the so-called “signal velocity,” the speed at which information propagates and that cannot exceed c .

DOI: 10.1103/PhysRevLett.93.203902

PACS numbers: 42.81.Gs, 42.25.Bs

The physics of light propagation is a very timely topic because of its relevance for both classical [1] and quantum [2] communication. Two kind of velocities are usually introduced to describe the propagation of a wave in a medium with dispersion $\omega(k)$: the phase velocity $v_{ph} = \frac{\omega}{k}$ and the group velocity $v_g = \frac{\partial\omega}{\partial k}$. Both of these velocities can exceed the speed of light in vacuum c in suitable cases [3]; hence, neither can describe the speed at which the information carried by a pulse propagates in the medium. Indeed, since the seminal work of Sommerfeld, extended and completed by Brillouin [4], it is known that information travels at the *signal velocity*, defined as the speed of the front of a square pulse. This velocity cannot exceed c [5]. The fact that no modification of the group velocity can increase the speed at which information is transmitted has been directly demonstrated in a recent experiment [6]. Superluminal (or even negative) and, on the other extreme, exceedingly small group velocities, have been observed in several media [7]. In this letter we report observation of both superluminal and delayed pulse propagation in a tabletop experiment that involves only a highly birefringent optical fiber and other standard telecommunication devices.

Before describing our setup, it is useful to understand in some more detail the mechanism through which anomalous group velocities can be obtained. For a light pulse sharply peaked in frequency, the speed of the center of mass is the group velocity v_g of the medium for the central frequency [3]. In the absence of anomalous light propagation, the local refractive index of the medium is n_f , supposed independent on frequency for the region of interest. The free propagation simply yields $v_g = L/t_f$ where L is the length of the medium and $t_f = n_f L/c$ is the free propagation time. One way to allow fast-light and slow-light amounts to modify the properties of the medium in such a way that it becomes opaque for all but the fastest (slowest) frequency components. The center of mass of the outgoing pulse appears then at a time $t = t_f + \langle t \rangle$, with $\langle t \rangle$ the mean time of arrival once the free propagation has been subtracted; obviously $\langle t \rangle < 0$ for fast light, $\langle t \rangle > 0$ for slow light. If the deformation of the pulse is weak, the group velocity is still the speed of

the center of mass, now given by

$$v_g = \frac{L}{t_f + \langle t \rangle}. \quad (1)$$

This can become either very large and even negative ($\langle t \rangle \rightarrow -\infty$) or very small ($\langle t \rangle \rightarrow \infty$)—although in these limiting situations the pulse is usually strongly distorted, so that our reasoning breaks down.

We can now move to our setup, sketched out in Fig. 1. The medium is a birefringent optical fiber of length L , whose refractive index is $n_f \approx \frac{3}{2}$ for the telecommunication wavelength 1550 nm. The fiber is sandwiched between two polarizers. This setup is also known in classical optics as a Lyot filter [8]. As shown in [9], this simple situation can be described with the quantum formalism of weak values [10]. In fact, the three essential ingredients of weak values are present here: (I) The input polarizer allows the *preselection* of a pure polarization state $|\psi_0\rangle$. (II) The birefringent fiber performs a *premeasurement* of polarization by spatially separating the two fibers' eigenmodes, supposed to be described by the eigenstates $|H\rangle$ and $|V\rangle$ of σ_z —that is, we choose z to be the birefringence axis. This premeasurement, known in telecommunication physics as polarization-mode dispersion (PMD), is weak whenever the temporal shift $\delta\tau$ [the so-called differential group delay, (DGD)] between the two eigenmodes of the fiber is much smaller than the coherence time t_c of the optical pulse. (III) The output polarizer performs the *postselection* on another chosen polarization state $|\phi\rangle$. The mean time of arrival of the optical pulse can be expressed as a function of a weak value W [1,9]:

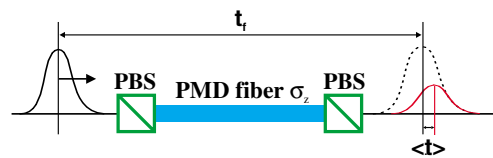


FIG. 1 (color online). Basic scheme. By carefully adjusting the direction of both PBS, one can modify the group velocity of the pulse.

$$\langle t \rangle = \frac{\delta\tau}{2} \text{Re}W = \frac{\delta\tau}{2} \text{Re} \left[\frac{\langle \phi | \sigma_z | \psi \rangle}{\langle \phi | \psi \rangle} \right] \quad (2)$$

where $|\psi\rangle$ is the polarization obtained by the free rotation of $|\psi_0\rangle$ in the fiber. Thus, $\langle t \rangle$ is in principle unbounded: by carefully choosing $|\psi_0\rangle$ and $|\phi\rangle$, i.e., the direction of each polarizer, one can tune the group velocity (1) to any desired value. In summary, by appending two polarizers at the ends of a birefringent fiber, one creates an *effective medium* whose dispersion and absorption properties depend on the pre- and postselection; in this effective medium, the group velocity can be increased or decreased by an arbitrary amount by merely choosing the orientations of two polarizers.

The rest of the paper is organized in three parts: first we derive the optical properties (dispersion and absorption) of our effective medium, stressing the role of the weak value W . Then we describe the experiment and present our main results in Figs. 4 and 5. We shall conclude by comparing our experiment to a related one [11], and by stressing the differences with other fast-light and slow-light techniques.

Theoretical analysis.—For any linear medium in which light propagates, the absorption coefficient $\kappa(\omega)$ and the index of refraction $n(\omega)$ are defined through

$$G(\omega) = e^{-\kappa(\omega)L} e^{i[n(\omega)\omega/c]L} \quad (3)$$

where L is the length of the fiber, and where $G(\omega)$ is the linear response function which characterizes the evolution of a plane wave of frequency ω in the medium: $e^{-i\omega t} \rightarrow G(\omega)e^{-i\omega t}$. The calculation of $G(\omega)$ for the effective medium sketched in Fig. 1 has to take polarization into account. The first polarizer prepares the state

$$|\psi_0\rangle \otimes e^{-i\omega t} = (a_0|H\rangle + b_0|V\rangle) \otimes e^{-i\omega t} \quad (4)$$

where $|H\rangle$ and $|V\rangle$ are the eigenmodes of the fiber, the eigenstates of the Pauli matrix σ_z for the eigenvalues ± 1 . As discussed in Ref. [9], the evolution of the polarization of the plane wave because of birefringence is given by the unitary operator $e^{i\omega\delta\tau\sigma_z/2}$, which describes a global rotation around the z axis of the Poincaré sphere—with our conventions, $|H\rangle$ is the slow mode and $|V\rangle$ is the fast mode. So, the state that reaches the second polarizer is $|\psi(\omega)\rangle \otimes e^{in_f\omega L/c} e^{-i\omega t}$ where one recognizes the phase acquired during free propagation through the fiber and where

$$|\psi(\omega)\rangle = a_0 e^{i(\delta\tau/2)\omega} |H\rangle + b_0 e^{-i(\delta\tau/2)\omega} |V\rangle. \quad (5)$$

The second polarizer is represented by the projector on a polarization state $|\phi\rangle = a_1|H\rangle + b_1|V\rangle$. So the output state reads $|\phi\rangle \otimes G(\omega)e^{-i\omega t}$ with a response function [12]

$$G(\omega) = e^{in_f\omega L/c} (A + B) \mathcal{F}(\omega, W_0) \quad (6)$$

where we have written $A \equiv a_1^* a_0$ and $B \equiv b_1^* b_0$, $\mathcal{F}(\omega, W_0) = \cos(\omega\delta\tau/2) + iW_0 \sin(\omega\delta\tau/2)$ and where

$$W_0 = \frac{A - B}{A + B} = \frac{\langle \phi | \sigma_z | \psi_0 \rangle}{\langle \phi | \psi_0 \rangle} \equiv W_R + iW_I \quad (7)$$

is the weak value involving the orientations of the two polarizers [13]. Note that this is not the weak value that enters the mean time of arrival (2): that one is computed using $|\psi(\omega)\rangle$ instead of $|\psi_0\rangle$; using (5), one obtains

$$W = \frac{W_R + i[W_I \cos\omega\delta\tau + \frac{1}{2}(1 - |W_0|^2) \sin\omega\delta\tau]}{|\mathcal{F}(\omega, W_0)|^2}. \quad (8)$$

From (3) and (6) it is straightforward to derive expressions for the absorption coefficient $\kappa(\omega)$ and the index of refraction $n(\omega)$. For simplicity, the global phases of both polarization states $|\psi_0\rangle$ and $|\phi\rangle$ are chosen such that $(A + B)$ is real and contributes thus only to the absorption. The results are

$$\kappa(\omega) = -\frac{1}{L} [\ln(A + B) + \ln|\mathcal{F}(\omega, W_0)|] \quad (9)$$

$$n(\omega) = n_f + \frac{c}{L\omega} \arctan \left[\frac{W_R}{\cot(\omega\delta\tau/2) - W_I} \right]. \quad (10)$$

From $n(\omega)$, one can derive the group index $n_g(\omega) = n + \omega \frac{dn}{d\omega}$. Using (8) and (2) one finds

$$n_g(\omega) = n_f + c \frac{\delta\tau}{2L} \text{Re}W = n_f + \frac{c}{L} \langle t \rangle. \quad (11)$$

This gives exactly the behavior (1) for the group velocity—indeed, both derivations are based on the assumption that the coherence time of the pulse is large compared to $\delta\tau$. When $\text{Re}W = \frac{W_R}{|\mathcal{F}(\omega, W_0)|^2}$ is small, the second term in (11) disappears and $n_g \approx n_f$: this is normal propagation, obtained for most choices of the pre- and postselection. The conditions $\text{Re}W = \pm 1$ are obtained for the slow and the fast polarization modes of the fiber, $|\psi_0\rangle = |H\rangle$ and $|V\rangle$, respectively. When $\text{Re}W > 1$, we obtain the slow-light regime; when $\text{Re}W < -1$, the fast-light regime. In particular, since $n_f \approx \frac{3}{2}$, superluminal group velocity ($n_g < 1$) requires $\text{Re}W < -\frac{c}{\delta\tau}$, negative group velocity ($n_g < 0$) requires $\text{Re}W < -3\frac{L}{c\delta\tau}$.

In Fig. 2, the absorption coefficient (9) and the index of refraction (10) are plotted for different weak values. When W_R increases, the slope of the index of refraction becomes steeper: a larger positive (negative) group delay

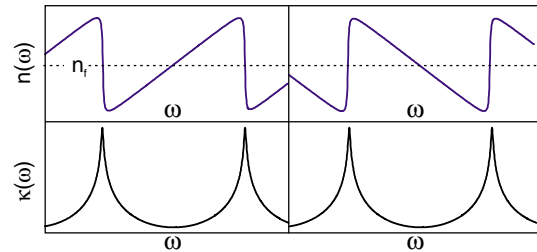


FIG. 2 (color online). Index of refraction and absorption coefficient versus frequency for $W_0 = W_R = \pm 6.0$.

corresponds to a slower (faster) group velocity. It is also clear from Fig. 2 that a strong absorption occurs whenever the change in the group velocity is important. Although these features are usual in their qualitative formulation, we note (as the authors of Ref. [11] did) that the standard Kramers-Kronig relations do not apply: these relations predict that the absorption coefficient ("imaginary part of the index") determines uniquely the index of refraction ("real part"), and vice versa; while in our case, the same absorption is associated with different dispersions. Modified Kramers-Kronig relations have been discussed in [14]. However, a full study of the question lies beyond the approach presented here, because our Equation (6) for $G(\omega)$ is valid only in a limited frequency range—e.g., the index of the fiber is not constant over all possible frequencies.

Experiment.—The experimental setup is sketched out in Fig. 3. As a source and for detection we use an optical time domain reflectometer (OTDR). This is a telecommunication instrument designed to measure loss profiles of fibers: it sends short laser pulses and analyzes the amount of back-scattered light as a function of time. Here we use a commercial prototype OTDR working in photon counting mode at the telecommunication wavelength $\lambda = 1.55 \mu\text{m}$ [15]. It contains a pulsed distributed-feedback laser (DFB) ($\Delta\nu \approx 500 \text{ MHz}$, pulse duration 2 ns) and a gated Peltier-cooled InGaAs photon counter (gate duration 2 ns). The photon counting OTDR is well adapted to this experiment since it allows to monitor the optical pulse, even in the presence of strong absorption. The birefringent fiber is a polarization maintaining (PM) fiber of length $L = 1.5 \text{ m}$, with a DGD $\delta\tau = 2.66 \text{ ps}$, measured with an interferometric low-coherence method [16]. The fiber is placed between two polarizing beam splitter (PBS) cubes with specified extinction ratios of 50 dB. Both cubes are mounted on rotational stages, allowing a precise alignment of pre- and postselected polarization states. Furthermore a micrometer step motor permits to slightly change the length of the fiber. This allows alignment of the postselection also in the x - y plane of the Poincaré sphere, since polarization is rotating around the z axis in the fiber.

The crucial part of the experiment is the alignment of both PBS cubes. The input polarizer has to be aligned at 45° relative to the fiber's axis [17]. This is done by injecting incoherent light (from a light-emitting diode) into the system and minimizing the degree of polarization at the output of the PM fiber. For the postselection, the position of the second PBS cube and the length of the

fiber are adjusted such that transmission through the system is minimum.

A first set of results is presented in Fig. 4. Figure 4(a) shows the data of a sequence of successive measurements on a dB scale. The largest curve is the reference pulse, i.e., the pulse in the normal regime, without any specific alignment of the PBS cubes. Between each measurement the postselection is slightly changed, in order to decrease transmission: we observe that the lower the transmission, the higher the group velocity, in agreement with the theory. In addition, Fig. 4(a) clearly illustrates the difference between group and signal velocities [4]. In fact, even though the group velocity is higher for each successive curve, the signal velocity remains constant and equal to c/n_f , since the front parts of all pulses are strictly identical. Figs. 4(b) and 4(c) show, respectively, a fast-light and a slow-light example. The measured data are plotted together with the reference pulse (dashed curve) and a fit (smooth solid curve). The fit is obtained by applying the following transformation to the reference pulse $I_{in}(t)$: $I_{in}(t) \rightarrow A_{in}(t) = \sqrt{I_{in}(t)} \xrightarrow{\text{FFT}} A_{in}(\omega) \rightarrow A_{out}(\omega) = G(\omega)A_{in}(\omega) \xrightarrow{\text{FFT}} A_{out}(t) \rightarrow I_{out}(t) = |A_{out}(t)|^2$, where FFT is a discrete Fourier-transform procedure. The first step of this fitting procedure assumes the reference pulse to be Fourier-transform limited; the slight discrepancies found between the data and the fits (in the front and back parts of the pulses) are

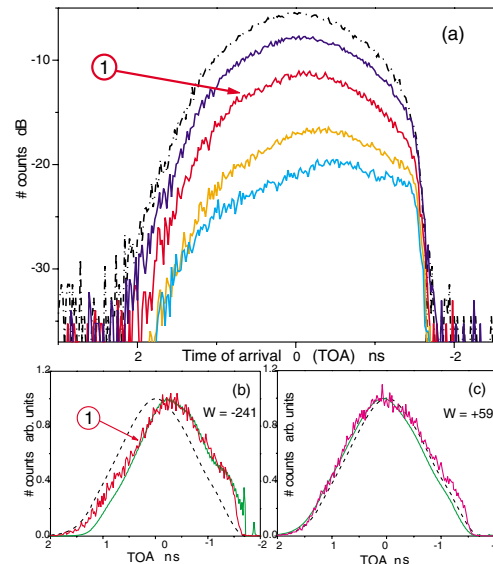


FIG. 4 (color online). In the three figures, the reference pulse (dashed line) has been normalized for convenience. (a) Sequence of measurements obtained by varying the orientation of a polarizer, in a log scale. The stronger the absorption, the larger the group velocity, as expected. However, the pulse is distorted in such a way that its front travels with a constant speed, the signal velocity c/n_f . (b), (c) Examples of measurements of fast light and of slow light, in a linear scale, together with theoretical fits (smooth solid curve). The real weak value W obtained from the fit is given.

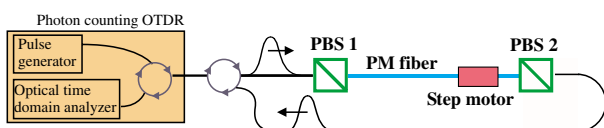


FIG. 3 (color online). Experimental setup.

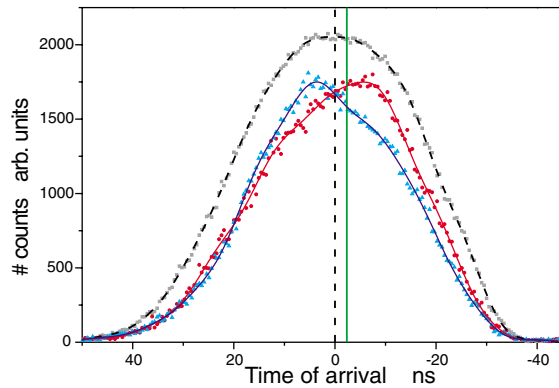


FIG. 5 (color online). Fast-light and slow-light curves compared to the reference pulse, whose center is marked by the dashed vertical line. The solid vertical line marks the position of the summit of a pulse that would have travelled at speed c . The fast pulse shows superluminal group velocity.

probably due to this approximation. The fitting parameter is the weak value W , supposed to be real. Note that in 4(b), $|W|$ lies below $\frac{1}{c\delta\tau} \approx 2000$, the value needed in order to demonstrate superluminal group velocity. To reach that bound, much longer input pulses are needed. We replace the OTDR source by an external source: a DFB laser ($\Delta\nu \approx 2$ MHz) working in continuous wave mode, modulated by an external electro-optic modulator. This source creates nearly Gaussian pulses with a coherence time of about 50 ns. The OTDR is still used for detection and triggers the modulator. Results are presented in Fig. 5. The pulse on the right shows clearly superluminal group velocity. By fitting the position of the maximum of the output pulse [18], we find $W \approx -3500$, consistent with superluminal but non-negative group velocity, as expected.

Comparison with other experiments.—Solli and co-workers reported on a similar, but indirect, experiment using polarized microwaves and a photonic crystal as birefringent medium, with identical conclusions on the group velocity [11]. Their conclusions were extracted from phase measurements only, so, in particular, they had no result on the signal velocity.

Most experiments on slow light have been performed using electromagnetically induced transparency (EIT) [7,19]. In EIT, the mode that carries information can be transmitted without losses, which is not the case in our experiment.

In conclusion, we presented an easy way to create slow and fast light using a birefringent optical fiber and other standard telecommunication components. The theoretical part of this work was mainly devoted to the study of the linear response function of our system $G(\omega)$, which is determined by a weak value, thus extending the previous work of [9]. In the experiment, we obtained clear evidence for superluminal group velocities (Fig. 5); we also

gave the first direct measurement of the signal velocity [Fig. 4(a)], showing that the increase of the group velocity does not increase the speed at which information travels.

We thank C. Barreiro for technical support. This work was supported by the Swiss NCCR “Quantum photonics.”

-
- [1] B. Huttner, C. Geiser, and N. Gisin, *IEEE J. Sel. Top. Quantum Electron.* **6**, 317 (2000).
 - [2] *The Physics of Quantum Information*, edited by D. Bouwmeester, A. Ekert, and A. Zeilinger (Springer, Berlin, 2000).
 - [3] J. D. Jackson, *Classical Electrodynamics*, (Wiley, New-York, 1975), 2nd ed., Sect. 7.
 - [4] L. Brillouin, *Wave Propagation and Group Velocity* (Academic Press, New-York, 1960).
 - [5] Actually, some weak excitations called “forerunners” may arrive even before the main front, but not faster than c . Their speed has been called, somehow unfortunately, “front velocity”.
 - [6] M. D. Stenner, D. J. Gauthier and M. Neifeld, *Nature (London)* **425**, 695 (2003).
 - [7] R. W. Boyd and D. J. Gauthier in *Progress in Optics*, edited by E. Wolf (Elsevier, Amsterdam, 2002), Vol. 43.
 - [8] W. Demtröder, *Laser spectroscopy* (Springer, Berlin, 2003).
 - [9] N. Brunner, A. Acín, D. Collins, N. Gisin, and V. Scarani, *Phys. Rev. Lett.* **91**, 180402 (2003).
 - [10] For a review see: Y. Aharonov and L. Vaidman, quant-ph/0105101; published in: *Time in Quantum Mechanics*, edited by J. G. Muga, R. Sala Mayato, and I. L. Egusquiza, Lecture Notes in Physics (Springer, Berlin, 2002).
 - [11] D. R. Solli, C. F. McCormick, C. Ropers, J. J. Morehead, R. Y. Chiao, and J. M. Hickmann, *Phys. Rev. Lett.* **91**, 143906 (2003).
 - [12] We have found a scalar response function $G(\omega)$ because we have preselected and postselected on pure polarization states. In general, the response function $G_{ij}(\omega)$ will be tensorial, relating the polarization components [11].
 - [13] A more complex link between response functions and weak values in a similar situation was pointed out in: D. R. Solli, C. F. McCormick, R. Y. Chiao, S. Popescu, and J. M. Hickmann, *Phys. Rev. Lett.* **92**, 043601 (2004).
 - [14] J. S. Toll, *Phys. Rev.* **104**, 1760 (1956).
 - [15] M. Wegmüller, F. Scholder, and N. Gisin, *J. Lightwave Technol.* **22**, 390 (2004).
 - [16] N. Gisin, J. P. Pellaux, and J. P. von der Weid, *IEEE LTS* **9**, 821 (1991)
 - [17] It can be easily shown from (2) that this preselection maximizes the mean time of arrival $\langle t \rangle$.
 - [18] We were not able to correctly fit the shape of these curves. This is probably due to a saturation of the OTDR detection or to some phase noise that invalidates the first step of the fitting procedure.
 - [19] S. Harris, *Phys. Today*, **50**, 36 (1997); M. D. Lukin and A. Imamoglu, *Nature (London)* **413**, 273 (2001).